A Galilean Invariant Explicit Algebraic Reynolds Stress Model For Curved Flows

*Sharath S. Girimaji**

Institute for Computer Applications in Science and Engineering

NASA Langley Research Center, Hampton, VA 23681

Abstract

A Galilean invariant weak-equilibrium hypothesis that is sensitive to streamline curvature is proposed. The hypothesis leads to an algebraic Reynolds stress model for curved flows that is fully explicit and self-consistent. The model is tested in curved homogeneous shear flow: the agreement is excellent with Reynolds stress closure model and adequate with available experimental data.

*This research was supported by the National Aeronautics and Space Administration under NASA Contract No. NAS1-19480 while the author was in residence at the Institute for Computer Applications in Science and Engineering (ICASE), NASA Langley Research Center, Hampton, VA 23681.

1 Introduction

Many turbulent flows of practical importance are characterized by curved streamlines: e.g., flow through turbines, curved pipes and channels, flows over wing sections and swirling flows. The qualitative effects of streamline curvature on turbulence are known from direct numerical simulations and experiments. Concave curvature, which is characterized by decreasing angular momentum with radius, gives rise to Taylor-Gortler instability in the flow resulting in increased velocity fluctuations and an augmentation of turbulence. Convex curvature, wherein angular momentum increases with radial distance, attenuates the Tollmien-Schlichting waves in boundary layers resulting in a decrease of turbulence. The quantitative effect of streamline curvature on turbulence is generally more profound than can be explained by a simple scaling analysis (Bradshaw [1], [2], Muck *et al.* [3] and Hoffman *et al.* [4]). Therefore, accurate modeling of the effect of streamline curvature on turbulence is very important.

Currently, the full Reynolds stress closure approach offers the most accurate means of calculating curved flows. Despite advances in computer capabilities, the Reynolds stress closure is still computationally too expensive for many engineering calculations of complex flows. Current engineering calculations employ, at best, two-equation turbulence models. At the two-equation level of turbulence modeling, algebraic Reynolds stress models derived from the Reynolds stress transport equation offer the most sophistication. In slowly evolving turbulent rectilinear flows, which form an important class of engineering flows, the algebraic Reynolds stress model can be considered as the solution of the Reynolds stress transport equation. In these flows, the algebraic Reynolds stress model offers the sophistication of the Reynolds stress closure approach at a much smaller computational expense. While being adequate for non-curved flows, current two-equation models are not accurate to even within engineering accuracy for curved flows. The development of an algebraic Reynolds stress model that is the formal solution to the transport equation in slowly evolving curved flows would constitute an important contribution and such is the intent of this paper.

1.1 Algebraic Reynolds stress modeling

The derivation of an algebraic Reynolds stress model from the differential transport equation is possible in the weak- or structural- equilibrium limit of turbulence where the anisotropy of Reynolds stress

$$b_{ij} \equiv \frac{\overline{u_i u_j}}{2K} - \frac{2}{3}\delta_{ij} \tag{1}$$

is approximately constant following a fluid particle:

$$\frac{\partial b_{ij}}{\partial t} + U_k (b_{ij})_{,k} \approx 0, \tag{2}$$

where, $\overline{u_i u_j}$ is the Reynolds stress, K is the turbulent kinetic energy, δ_{ij} is the Kronecker delta and the comma in the subscript indicates total derivative (including Christoffel symbol terms) with respect to the index direction. (Throughout this paper, an upper case symbol indicates the mean of a quantity and lower case represents the fluctuation from the mean.) This weak-equilibrium assumption was first invoked by Rodi [5] and the accuracy of the algebraic Reynolds stress model for a given flow depends upon the degree of validity of the assumption in that flow.

The Reynolds stress anisotropy evolution equation, on invoking the weak-equilibrium assumption, reduces to a set of nonlinear algebraic equations. All of the algebraic modeling methodologies to date (e.g., Rodi [5], Pope [6], Taulbee [7], Gatski and Speziale [8] and Girimaji [9]) attempt to solve these equations for the Reynolds stress anisotropy. The algebraic Reynolds stress models can be classified as implicit or explicit. The implicit models ([5], [6], and [7]) solve the non-linear equations numerically, in an iterative fashion, which could (i) be computationally expensive and (ii) converge to non-physical real roots leading to serious errors in the calculations. The explicit algebraic model of Gatski and Speziale [8] is an analytical solution to the algebraic equations linearized about the equilibrium state of homogeneous turbulence. While this model works quite well near equilibrium, when used away from equilibrium (as most practical models invariably are), it leads to inconsistency between the assumed equilibrium value of the P/ε ratio and the derived value of the Reynolds stress anisotropy (Girimaji [9]). The algebraic model of Girimaji [9] is obtained by analytically solving the algebraic equations for anisotropy in their fully nonlinear form;

this model is both fully explicit *and* self-consistent. This model expression is the exact fixed point solution (i.e., in the weak equilibrium limit) of the Reynolds stress transport equation in two-dimensional mean flows for a variety of quasilinear pressure-strain correlation models.

The Rodi weak-equilibrium assumption and circular flows. In fully developed curved flows with circular streamlines, the anisotropy of Reynolds stress does not change following a streamline (Eskinazi and Yeh [10], Moser and Moin [11]):

$$\frac{\partial b_{ij}^s}{\partial t} + U_k^s \frac{\partial b_{ij}^s}{\partial x_k^s} \approx 0, \tag{3}$$

where x_i^s is a streamline coordinate. For curved flows, it is easily seen that the Rodi weak-equilibrium simplification (equation 2) is inconsistent with the above observation (equation 3). The inconsistency is most easily seen in the streamline coordinate system where the Rodi assumption implies

$$\frac{\partial b_{ij}^s}{\partial t} + U_k^s \frac{\partial b_{ij}^s}{\partial x_k^s} = \text{Christoffel symbol terms} \neq 0. \tag{4}$$

Therefore, the Rodi weak-equilibrium assumption and the algebraic Reynolds stress models derived using it are not suited for curved turbulent flows.

Streamline weak-equilibrium assumption for curved flows. Some authors (e.g., Rodi and Scheurer [12] designated RS, and Younis [13]) have hypothesized that, in curved flows, the anisotropy following a streamline is constant (equation 3). This streamline weak-equilibrium assumption is used to reduce the anisotropy transport equation to a set of non-linear algebraic equations. The resulting ARSM has yielded somewhat improved performance for curved flows. However, the streamline weak-equilibrium assumption (equation 3) depends on the streamline direction, which in turn depends on the fluid velocity. In general, the fluid velocity is not Galilean invariant. As a consequence, the streamline direction and, therefore, the streamline weak-equilibrium assumption is not Galilean invariant (Girimaji [14], Fu *et al.* [15]). Fu *et al.* suggest that the Galilean variance may be the reason for the poor performance of ARSM in their curved flow computations.

The current status of the algebraic stress model for curved flows is the following: *The streamline weak-equilibrium assumption (equation 3) which is suitably sensitive to curvature is not Galilean invariant. The Rodi weak-equilibrium assumption (equation 2) is Galilean invariant but not properly sensitive to streamline curvature.*

Present work. The first and the most important objective of this paper is the construction of a new weak-equilibrium hypothesis that is (i) Galilean invariant, (ii) properly sensitive to streamline curvature, and (iii) equivalent to the Rodi assumption in flows with rectilinear streamlines. The second objective is to derive an algebraic model expression for the Reynolds stress anisotropy that is (i) fully explicit, (ii) self-consistent, (iii) Galilean invariant, and (iv) sensitive to streamline curvature.

The remainder of the paper is organized as follows. The new weak-equilibrium assumption is proposed in Section 2. The Reynolds stress transport equation is reduced to a set of nonlinear algebraic equations in Section 3. A fully explicit and self-consistent algebraic model expression for anisotropy is also presented. The model validation is performed in Section 4 and we conclude in Section 5.

2 Galilean invariant weak-equilibrium assumption

Invoking the weak-equilibrium assumption in the streamline coordinate system ($\mathbf{e}_i^s$) is ill-advised because the basis of the streamline coordinate system is the velocity vector which is not Galilean invariant. Unlike velocity, the acceleration vector $\frac{d}{dt}\mathbf{U}$ is Galilean invariant. If the weak equilibrium assumption is made in a coordinate system that is defined using the acceleration vector, a Galilean invariant model will result. The derivation given in this section employs three coordinate systems: acceleration coordinate system $\mathbf{e}_i^a$, streamline coordinate system $\mathbf{e}_i^s$, and an arbitrary computational coordinate system $\mathbf{e}_i$. The acceleration and the streamline coordinate systems are denoted by superscripts a and s respectively.

The *acceleration coordinate system* $\mathbf{e}_i^a$ is defined as follows. Let $\mathbf{a}$ be the unit vector in the direction of acceleration ($\frac{d}{dt}\mathbf{U}$). Let $\mathbf{e}_1^a$ be along $\mathbf{a}$ and let $\mathbf{e}_2^a$ be orthogonal to $\mathbf{a}$ on the plane of $\mathbf{a}$. Finally, define $\mathbf{e}_3^a$ normal to the plane of $\mathbf{a}$-field (unit binormal vector) completing an orthogonal right handed

system. In general, the streamline and the acceleration coordinate systems are different. However, when the mean fluid trajectory is circular, the acceleration (radial direction) is perpendicular to the velocity (tangential direction): the unit vectors of the acceleration and the streamline coordinate systems coincide. The *computational coordinate system* is an arbitrary orthogonal reference system in which the model calculations are performed. Our objective is to derive the final form of the model in the computational coordinate system. If a flow with circular streamlines is computed in a cylindrical coordinate system, the acceleration, streamline, and computational coordinate systems will coincide.

2.1 The new weak-equilibrium hypothesis

If the streamlines are perfectly circular, then the $\mathbf{e}_i^a$ coordinate system will coincide with the streamline coordinate system, leading to

$$\frac{\partial b_{ij}^a}{\partial t} + U_l^a \frac{\partial b_{ij}^a}{\partial x_l^a} = \frac{\partial b_{ij}^s}{\partial t} + U_k^s \frac{\partial b_{ij}^s}{\partial x_k^s} = 0. \tag{5}$$

When the fluid motion is non-circular in the computational coordinate system $\mathbf{e}_i$ (i.e., velocity and acceleration are not orthogonal), we can perform a Galilean transformation to a new moving coordinate frame in which the fluid acceleration is unchanged (since it is Galilean invariant) while the direction of the fluid velocity changes. If the reference frame velocity is chosen appropriately, the fluid velocity and acceleration can be made orthogonal to one another. Clearly, this frame transformation is a function of space and time. In this new coordinate frame, the fluid motion is locally circular. Locally, the radial, tangential, and axial directions of this circular flow are the $\mathbf{e}_1^a$, $\mathbf{e}_2^a$, and $\mathbf{e}_3^a$ directions, respectively. Based upon our knowledge of circular flows (equation 5), we now hypothesize that along these coordinate directions the anisotropy of Reynolds stress is invariant leading to:

$$\frac{\partial b_{ij}^a}{\partial t} + U_l^a \frac{\partial b_{ij}^a}{\partial x_l^a} \approx 0. \tag{6}$$

Let us investigate how the above hypothesis satisfies the three required criteria listed in the Introduction.

1. The hypothesis depends only upon the direction of the acceleration vector and, hence, is Galilean invariant.

2. For circular flows, it is clear (equation 5) that anisotropy is invariant following the streamline.

3. In the absence of streamline curvature, the Lagrangian velocity is unidirectional; the direction of acceleration is invariant. The acceleration coordinate system can be taken to be a Cartesian coordinate system. Then, the present simplification (equation 6) reduces to the Rodi weak-equilibrium assumption (Criterion 3).

For these reasons, the hypothesis given in equation (6) appears to be a reasonably sound foundation for building an algebraic Reynolds stress model for general curved flows.

Hypothesis in the computational coordinate system. Computations are seldom performed in the acceleration coordinate system $\mathbf{e}_i^a$. For the new weak-equilibrium assumption to be useful, it is necessary to express equation (6) in the arbitrary orthogonal computational coordinate system ($\mathbf{x}$, t) whose unit vectors are $\mathbf{e}_i$. If T_{ip} is the transformation matrix between the acceleration and the computational coordinate systems, we have the following relationships:

$$\begin{aligned} \mathbf{e}_i^a &= T_{ip}\mathbf{e}_p; \quad \mathbf{e}_p = T_{ip}\mathbf{e}_i^a; \quad U_i^a = T_{ip}U_p \\ b_{ij}^a &= T_{ip}T_{jq}b_{pq}; \quad T_{ip}T_{jp} = \delta_{ij}. \end{aligned} \tag{7}$$

The elements of the transformation matrix are known once the acceleration vector is known in the $\mathbf{e}_i$ coordinate system. If the mean flow is two-dimensional (many flows of practical interest fall into this category), T_{ip} can be easily calculated. Letting $\mathbf{e}_1$ and $\mathbf{e}_2$ be the coordinates along which the flow varies, and $\mathbf{e}_3$ be the homogeneous direction, we have

$$\begin{aligned} e_1^a &= a_1e_1 + a_2e_2, \\ e_2^a &= -a_2e_1 + a_1e_2, \\ e_3^a &= e_3, \end{aligned} \tag{8}$$

where $\mathbf{a}$ is the unit vector in the direction of acceleration. For this case, $\mathbf{T}$ is given by

$$T_{ij} = \begin{pmatrix} a_1 & a_2 & 0 \\ -a_2 & a_1 & 0 \\ 0 & 0 & 1 \end{pmatrix}.$$

The anisotropy tensor can now be expressed as

$$\mathbf{b} \equiv b^a_{ij}\mathbf{e}^a_i\mathbf{e}^a_j \equiv b_{ij}\mathbf{e}_i\mathbf{e}_j. \tag{9}$$

Invoking the new weak-equilibrium assumption (6), we can write

$$\begin{aligned} \frac{\partial \mathbf{b}}{\partial t} + U^a_l \frac{\partial \mathbf{b}}{\partial x^a_l} &= [\frac{\partial b^a_{ij}}{\partial t} + U^a_l \frac{\partial b^a_{ij}}{\partial x^a_l}]\mathbf{e}^a_i\mathbf{e}^a_j + b^a_{ij}[\frac{\partial \mathbf{e}^a_i\mathbf{e}^a_j}{\partial t} + U^a_l \frac{\partial \mathbf{e}^a_i\mathbf{e}^a_j}{\partial x^a_l}] \\ &\approx b^a_{ij}[\frac{\partial \mathbf{e}^a_i\mathbf{e}^a_j}{\partial t} + U^a_l \frac{\partial \mathbf{e}^a_i\mathbf{e}^a_j}{\partial x^a_l}] \\ &= b^a_{ij}[\frac{\partial \mathbf{e}^a_i\mathbf{e}^a_j}{\partial t} + U_l \frac{\partial \mathbf{e}^a_i\mathbf{e}^a_j}{\partial x_l}]. \end{aligned} \tag{10}$$

The invariance property of $U_l(\partial/\partial x_l)$ is used to write the last equality in the above equation.

Using equation (7) we can write,

$$\mathbf{e}^a_i\mathbf{e}^a_j = T_{ip}T_{jq}\mathbf{e}_p\mathbf{e}_q. \tag{11}$$

Define the temporal and spatial derivatives of the computational coordinate system as follows:

$$F_{pq} = \frac{\partial \mathbf{e}_p}{\partial t}(.)\mathbf{e}_q; \quad \Gamma_{plq} = \frac{\partial \mathbf{e_p}}{\partial x_l}(.)\mathbf{e}_q, \tag{12}$$

where, (.) denotes inner product. Like the Christoffel symbol, Γ is a coupling function. Now we can write

$$\begin{aligned} \frac{\partial \mathbf{e}^a_i\mathbf{e}^a_j}{\partial t} + U_l \frac{\partial \mathbf{e}^a_i\mathbf{e}^a_j}{\partial x_l} &= T_{ip}T_{jq}[\frac{\partial \mathbf{e}_p\mathbf{e}_q}{\partial t} + U_l \frac{\partial \mathbf{e}_p\mathbf{e}_q}{\partial x_l}] + \mathbf{e}_p\mathbf{e}_q[\frac{\partial}{\partial t}(T_{ip}T_{jq}) + U_l \frac{\partial}{\partial x_l}(T_{ip}T_{jq})] \\ &= \mathbf{e}_p\mathbf{e}_q[T_{ir}T_{jq}(F_{rp} + U_l\Gamma_{rlp}) + T_{ip}T_{jr}(F_{rq} + U_l\Gamma_{rlq}) + \frac{d}{dt}(T_{ip}T_{jq})], \end{aligned} \tag{13}$$

where $d/dt = (\partial/\partial t) + U_l(\partial/\partial x_l)$.

By employing equation (13) and the following identities

$$b^a_{ij}T_{ir}T_{jq} = b_{rq}; \;\; b^a_{ij}T_{ip}T_{jr} = b_{pr}; \;\; b^a_{ij} = b_{rs}T_{ir}T_{js}, \tag{14}$$

the weak-equilibrium approximation (equation 10) can now be written in the computational coordinate system:

$$\frac{\partial \mathbf{b}}{\partial t} + U_l \frac{\partial \mathbf{b}}{\partial x_l} = \mathbf{e}_p \mathbf{e}_q [b_{rq}(F_{rp} + U_l \Gamma_{rlp}) + b_{pr}(F_{rq} + U_l \Gamma_{rlq}) + b_{rs} T_{ir} T_{js} (T_{jq} \frac{dT_{ip}}{dt} + T_{ip} \frac{dT_{jq}}{dt})]. \quad (15)$$

In component form, the weak-equilibrium approximation in the computational coordinate system is

$$\begin{aligned} \frac{\partial b_{pq}}{\partial t} + U_l (b_{pq})_{,l} &= b_{rq}(F_{rp} + U_l \Gamma_{rlp}) + b_{pr}(F_{rq} + U_l \Gamma_{rlq}) + b_{rs} T_{ir} T_{js} (T_{jq} \frac{dT_{ip}}{dt} + T_{ip} \frac{dT_{jq}}{dt}) \quad (16) \\ &= b_{pr} \Omega'_{rq} + b_{qr} \Omega'_{rp}. \end{aligned}$$

In the above equations, Ω'_{rs} is an antisymmetric tensor given by

$$\Omega'_{rs} = F_{rs} + U_l \Gamma_{rls} + T_{qr} \frac{dT_{qs}}{dt}. \quad (17)$$

If the computational coordinate system is time-invariant, then $F_{rs} = 0$. If the computational coordinate system is Cartesian, then $\Gamma_{rls} = 0$. If the mean flow streamline is perfectly circular and the streamline coordinate system is used, then $T_{rs} = \delta_{rs}$, leading to $d/dt(T_{rs}) = 0$.

3 Model development

In this section, the new weak-equilibrium assumption is employed to develop an explicit algebraic Reynolds stress model that is appropriate for curved flows.

The exact Reynolds stress transport equation in an arbitrary inertial reference frame is given by

$$\frac{\partial \overline{u_i u_j}}{\partial t} + U_k (\overline{u_i u_j})_{,k} + (\overline{u_i u_j u_k})_{,k} = P_{ij} + \varepsilon_{ij} + \phi_{ij} + \mathcal{D}_{ij}. \quad (18)$$

The terms, respectively, are the time rate of change, advection, turbulent transport, production (P_{ij}), dissipation (ε_{ij}), pressure-strain correlation (ϕ_{ij}), and pressure-viscous diffusion ($\mathcal{D}_{ij}$) of the Reynolds stress:

$$\begin{aligned} P_{ij} &= -\overline{u_i u_k} U_{j,k} - \overline{u_j u_k} U_{i,k}; \quad \varepsilon_{ij} = 2\nu \overline{u_{i,k} u_{j,k}} \quad (19) \\ \mathcal{D}_{ij} &= [-\overline{p u_i} \delta_{jl} - \overline{p u_j} \delta_{il} + \nu \overline{u_i u_j}_{,l}]_{,l}. \end{aligned}$$

The production and dissipation rate of turbulent kinetic energy are, respectively, $P = \frac{1}{2}P_{ii}$ and $\varepsilon = \frac{1}{2}\varepsilon_{ii}$. The dissipation rate tensor can be split into its isotropic and deviatoric parts: $\varepsilon_{ij} = \frac{2}{3}\varepsilon\delta_{ij} + d_{ij}$. The transport equation for the anisotropy tensor in non-dimensional time is derived from equation (18) (see Girimaji [9]):

$$\frac{\partial b_{ij}}{\partial t'} + U_l(b_{ij})_{,l} + b_{ij}(\frac{P}{\varepsilon} - 1) = -\frac{2}{3}S_{ij} - (b_{ik}S_{kj} + S_{ik}b_{kj} - \frac{2}{3}b_{mn}S_{mn}\delta_{ij}) - (b_{ik}\omega_{jk} + b_{jk}\omega_{ik}) + \frac{1}{2}\Pi^*_{ij}. \quad (20)$$

In the above equation the following normalizations have been effected using the eddy turnover time:

$$\begin{aligned} \partial t' &= \frac{\varepsilon}{K}\partial t; \quad S_{ij} = \frac{1}{2}\frac{K}{\varepsilon}(U_{i,j} + U_{j,i}); \\ \omega_{ij} &= \frac{1}{2}\frac{K}{\varepsilon}(U_{i,j} - U_{j,i}); \quad \Pi^*_{ij} = \frac{K}{\varepsilon}(\phi_{ij} - d_{ij}). \end{aligned} \quad (21)$$

Invoking the weak equilibrium assumption (equation 16), the anisotropy transport equation in the computational coordinate system can be reduced to the following set of nonlinear algebraic equations:

$$b_{ij}(\frac{P}{\varepsilon} - 1) = -\frac{2}{3}S_{ij} - (b_{ik}S_{kj} + S_{ik}b_{kj} - \frac{2}{3}b_{mn}S_{mn}\delta_{ij}) - [b_{ik}(\omega_{jk} - \Omega_{jk}) + b_{jk}(\omega_{ik} - \Omega_{ik})] + \frac{1}{2}\Pi^*_{ij}, \quad (22)$$

where,

$$\Omega_{rs} = \frac{K}{\varepsilon}\Omega'_{rs}. \quad (23)$$

We consider the following type of quasilinear pressure-strain model (that includes all linear models):

$$\Pi^*_{ij} = -(C_1^0 + C_1^1\frac{P}{\varepsilon})b_{ij} + C_2S_{ij} + C_3(b_{ik}S_{jk} + b_{jk}S_{ik} - \frac{2}{3}b_{mn}S_{mn}\delta_{ij}) + C_4(b_{ik}\omega_{jk} + b_{jk}\omega_{ik}), \quad (24)$$

where the C's are numerical constants. Many of the current pressure-strain correlation models are special cases of equation (24) near weak-equilibrium. Using this model, the nonlinear set of simultaneous equations (22) for the anisotropy components is written in the following compact form:

$$b_{ij}[L_1^0 - L_1^1 b_{mn}S_{mn}] = L_2S_{ij} + L_3(b_{ik}S_{kj} + S_{ik}b_{kj} - \frac{2}{3}b_{mn}S_{mn}\delta_{ij}) + L_4(b_{ik}W_{jk} + b_{jk}W_{ik}), \quad (25)$$

where,

$$L_1^0 = \frac{C_1^0}{2} - 1; \;\; L_1^1 = C_1^1 + 2; \;\; L_2 = \frac{C_2}{2} - \frac{2}{3}; \;\; L_3 = \frac{C_3}{2} - 1; \;\; L_4 = \frac{C_4}{2} - 1. \quad (26)$$

The total effective vorticity W_{ij} is given by

$$W_{ij} = \omega_{ij} + \frac{2}{C_4 - 2}\Omega_{ij}. \tag{27}$$

This implies that the effect of streamline curvature is to modify the flow vorticity and, hence, Ω_{ij} is called the vorticity modification tensor. The effect of coordinate frame rotation also appears via a modified vorticity term (Gatski and Speziale [8], equation (26)). However, there is a major difference between the two phenomena: whereas, solid body rotation of the coordinate frame modifies flow vorticity by the same amount everywhere, the modification due to streamline curvature can vary with space and time.

The objective now is to solve equation (25) for b_{ij}. The solution – in terms of the constants L, strain rate S_{ij}, and effective vorticity W_{ij} – will produce the algebraic Reynolds stress model.

3.1 Fully-explicit solution

The set of nonlinear algebraic simultaneous equations for the anisotropy of Reynolds stress has the same form (equation 25) with or without streamline curvature. The only difference in the two cases would be the lack of vorticity modification in the rectilinear streamline case. For the case of straight streamlines, the solution of equation (25) has been derived by Girimaji [9]. The solution procedure presented in Girimaji [9] departs from those previously given in the literature by treating the algebraic equations in their full nonlinear form. The final solution, following a brief description of the derivation procedure, is now given.

Representation theory provides the most general tensorial form of the anisotropy tensor in terms of the strain and rotation rate tensors. For three-dimensional flows, the functional form is too cumbersome to be of practical value (Gatski and Speziale [8]). It is customary to restrict consideration to the more tractable case of two-dimensional mean flows and use the resultant functional form of the Reynolds stress expression as a model in three-dimensional flows also. For two-dimensional mean flows, the general admissible representation of the anisotropy tensor is given by

$$b_{ij} = G_1 S_{ij} + G_2(S_{ik}W_{kj} - W_{ik}S_{kj}) + G_3(S_{ik}S_{kj} - \frac{1}{3}S_{mn}S_{mn}\delta_{ij}). \tag{28}$$

(The tensor $W_{ik}W_{kj}$, which is also permitted by representation theory, is not admitted for it is inconsistent

with known physics, see Gatski and Speziale [8] for details). The unknown coefficients (eddy viscosities), $G_1 - G_3$, are functions of the constants of the pressure-strain model and the invariants of the strain and rotation rate tensors. In incompressible flows, these invariants are

$$\eta_1 = S_{ij}S_{ij}; \quad \eta_2 = W_{ij}W_{ij}. \tag{29}$$

It can be easily shown that the coefficient G_1 is related to the turbulent eddy viscosity coefficient, C_μ, commonly used in K-ε modeling:

$$C_\mu = -G_1. \tag{30}$$

The objective now is to determine the unknown coefficients by ensuring that the representation of anisotropy (28) satisfies equation (25). Equation (25) is nonlinear and has multiple roots. As a result, as demonstrated in Girimaji [9], G_1 has multiple representations. The only physically meaningful solution of equation (25) is selected by requiring that G_1 be (i) real, (ii) a continuous function of its parameters η_1 and η_2, and (iii) consistent with known physical behavior (Girimaji [9]):

$$G_1 = \begin{cases} L_1^0 L_2/[(L_1^0)^2 + 2\eta_2(L_4)^2], & \text{for } \eta_1 = 0; \\ L_1^0 L_2/[(L_1^0)^2 - \frac{2}{3}\eta_1(L_3)^2 + 2\eta_2(L_4)^2], & \text{for } L_1^1 = 0; \\ -\frac{p}{3} + (-\frac{b}{2} + \sqrt{D})^{\frac{1}{3}} + (-\frac{b}{2} - \sqrt{D})^{\frac{1}{3}}, & \text{for } D > 0; \\ -\frac{p}{3} + 2\sqrt{\frac{-a}{3}}cos(\frac{\theta}{3}), & \text{for } D < 0 \text{ and } b < 0; \\ -\frac{p}{3} + 2\sqrt{\frac{-a}{3}}cos(\frac{\theta}{3} + \frac{2\pi}{3}), & \text{for } D < 0 \text{ and } b > 0. \end{cases} \tag{31}$$

The various quantities in the above equation are given by

$$\begin{aligned} p &\equiv -\frac{2L_1^0}{\eta_1 L_1^1}; \quad r \equiv -\frac{L_1^0 L_2}{(\eta_1 L_1^1)^2}; \\ q &\equiv \frac{1}{(\eta_1 L_1^1)^2}[(L_1^0)^2 + \eta_1 L_1^1 L_2 - \frac{2}{3}\eta_1(L_3)^2 + 2\eta_2(L_4)^2]; \\ a &\equiv (q - \frac{p^2}{3}); \quad b \equiv \frac{1}{27}(2p^3 - 9pq + 27r); \\ D &= \frac{b^2}{4} + \frac{a^3}{27}; \quad cos(\theta) = \frac{-b/2}{\sqrt{-a^3/27}}. \end{aligned} \tag{32}$$

The other two coefficients G_2 and G_3 can be calculated as follows:

$$G_2 = \frac{-L_4 G_1}{L_0^1 - \eta_1 L_1^1 G_1}; \quad G_3 = \frac{2L_3 G_1}{L_0^1 - \eta_1 L_1^1 G_1}. \tag{33}$$

The turbulent diffusivity coefficient C_μ ($\equiv -G_1$) is plotted as a function of η_1 and η_2 in Figure 1. It is easily seen that this coefficient is a well-behaved and non-singular function of η_1 and η_2. The value of C_μ typically used in K-ε modeling is 0.09. It is seen from this figure that for moderate values of η_1 and η_2 the present model predicts a value of C_μ close to 0.09. At very high values of strain or rotation rate, the C_μ value tends to zero. For a given strain rate (η_1), C_μ decreases with increasing rotation rate (η_2). The two other coefficients are also well-behaved functions of η_1 and η_2 [9].

The expression for the anisotropy of Reynolds stress is fully explicit since the production to dissipation ratio (appearing as $b_{mn}S_{mn}$ in equation 25) is not treated quasistatically as done by Rodi [5], Pope [6] or Taulbee [7]. Also, this expression is self-consistent even far from equilibrium since equation (25) is solved in its fully nonlinear form, rather than by linearizing the equation about the equilibrium value as done by Gatski and Speziale [8]. The advantages of the current fully explicit model over previous models are discussed in Girimaji [9].

4 Discussion and comparison with experiment

In this section, we first discuss the validity of the algebraic Reynolds stress methodology in general curved inhomogeneous flows. Next, we discuss the similarities and differences between the present and the streamline weak-equilibrium (equation 3) assumptions. Finally, the explicit algebraic Reynolds stress model is examined in the simplest of curved flows – the curved homogeneous shear flow. The model evaluation is performed in two parts: comparison with other models; and validation against the homogeneous curved shear flow experimental data of Holloway and Tavoularis [17]. The testing of the model in more complex curved flows has been deferred to the future.

4.1 Validity in inhomogeneous flows

The derivation presented in the previous section is fully valid only in homogeneous flows. In inhomogeneous flows, upon the invocation of the weak-equilibrium assumption, the Reynolds stress anisotropy evolution equation is still not algebraic due to the presence of the viscous and turbulent transport terms. Therefore

the algebraic Reynolds stress methodology is formally valid only when the transport terms are negligible and the anisotropy evolution is completely determined by the local processes of production, pressure-strain correlation, and dissipation. In high Reynolds number flows, the viscous transport is generally negligible. We estimate the importance of the turbulent transport in curved flows using the experimental data of Muck *et al.* [3] and Hoffman *et al.* [4], and the direct numerical simulation data of Moser and Moin [11].

Convex curvature. The turbulent kinetic energy and shear stress budgets measured in convexly curved boundary layer indicate that the 'turbulent transport (by triple products and pressure fluctuations) and advection are both considerably decreased by the application of curvature' (Muck *et al.* [3]). Throughout the convexly curved boundary layer, the production and dissipation are much larger in magnitude than the other terms and nearly balance each other completely. In the curved channel flow of Moser and Moin [11], in the convex portion, the production, dissipation, and pressure-strain correlation of normal stresses are much larger than the turbulent transport. The shear stress evolution is predominantly determined by the balance between production and pressure-strain redistribution. It appears that the neglect of turbulent transport is a better approximation in convex flows than in straight flows. Therefore, the algebraic Reynolds stress methodology is at least as valid in convex flows as it is in straight flows.

Concave flows. The concave boundary layer data of Hoffman *et al.* [4] and the curved channel flow data of Moser and Moin [11] indicate that the turbulent transport terms are larger in concave flows than in straight flows. However, except at the very edge of the concave boundary layer, the production, dissipation, and pressure strain redistribution continue to be larger than the turbulent transport terms. Therefore, the algebraic Reynolds stress methodology is less valid in concave flows, but still adequate.

In the near wall region, for up to 20 wall units, the structure of the velocity field in convex and concave flows are identical to that of a straight flow ([3], [4], [11]). In this region, although turbulent transport is large, the production and dissipation are extremely large and dominate the flow dynamics. This appears to indicate that the near-wall treatment in curved flow calculations can be the same as in straight flows.

4.2 Present vs. streamline weak-equilibrium assumption

Apart from the fact that the present assumption is Galilean invariant whereas the streamline weak-equilibrium assumption is not, there are important physical differences between the two models. As mentioned earlier, the present weak-equilibrium assumption leads to the following vorticity modification:

$$\Omega'_{ij}(\text{present}) = F_{ij} + U_l \Gamma_{ilj} + T_{li} \frac{dT_{lj}}{dt}. \tag{34}$$

The term F_{ij} accounts for the unsteadiness of the curved flow, $U_l \Gamma_{ilj}$ arises due to the curvature of the computational coordinate system, and the last term on the right hand side is due to the changing direction of the acceleration (with respect to the computational coordinate system). It can be shown that the vorticity modification due to the streamline weak-equilibrium assumption is

$$\Omega'_{ij}(\text{streamline}) = U_l \Gamma_{ilj}. \tag{35}$$

For steady circular flows being computed in the cylindrical streamline coordinate system, the two weak-equilibrium assumptions are equivalent. However, the streamline weak-equilibrium model cannot account for the unsteadiness or varying direction of the acceleration. The latter feature is very important in steady curved (non-circular) flows. For example, in the transition from a straight to a curved channel turbulent flow (or *vice-versa*) the term containing T_{ij} is likely to be very important. One of the most important deficiencies of the streamline weak-equilibrium model is its inability to capture the recovery of turbulence from imposed streamline curvature, Rodi and Scheurer [12]. The previous curved flow models have also been shown to be inadequate in swirling flows. In these cases, the present model can be expected to perform better.

4.3 Model validation

For the sake of simplicity, in this paper, we restrict the model testing to curved homogeneous shear flow which is initially isotropic. The model is validated against other models and experimental data. This flow has circular streamlines and is characterized by the normalized shear rate and the curvature factor defined,

respectively, as

$$S = \frac{\partial U}{\partial r}\frac{K}{\varepsilon}; \quad C_f = (\frac{U}{r})/(\frac{\partial U}{\partial r}). \tag{36}$$

In these definitions, U is the tangential velocity and r is the radial coordinate. Let the 1, 2, and 3 directions correspond to the radial, tangential, and axial directions respectively. In this cylindrical coordinate system the only non-zero Christoffel terms are

$$\Gamma_{122} = \frac{1}{r}; \quad \Gamma_{211} = -\frac{1}{r}. \tag{37}$$

The non-dimensional mean strain-rate and vorticity are given by

$$S_{ij} = \frac{1}{2}S(1 - C_f)\begin{pmatrix} 0 & 1 & 0 \\ 1 & 0 & 0 \\ 0 & 0 & 0 \end{pmatrix}; \quad \omega_{ij} = \frac{1}{2}S(1 + C_f)\begin{pmatrix} 0 & -1 & 0 \\ 1 & 0 & 0 \\ 0 & 0 & 0 \end{pmatrix}. \tag{38}$$

The vorticity modification tensor is given by

$$\Omega_{ij} = \frac{2}{C_4 - 2}\frac{U}{r}\begin{pmatrix} 0 & 1 & 0 \\ -1 & 0 & 0 \\ 0 & 0 & 0 \end{pmatrix}. \tag{39}$$

By adding equation (39) to the mean flow vorticity tensor we obtain the non-dimensional total vorticity,

$$W_{ij} = \frac{S}{2}[1 + C_f + MC_f]\begin{pmatrix} 0 & -1 & 0 \\ 1 & 0 & 0 \\ 0 & 0 & 0 \end{pmatrix}, \tag{40}$$

where, M is the vorticity modification factor due to streamline curvature and is given by

$$M = -\frac{4}{C_4 - 2}. \tag{41}$$

In all of the major pressure-strain correlation models, the value of C_4 is less than two. Therefore, when the streamline curvature is convex ($C_f > 0$), the effect of curvature is to augment the vorticity. As was shown in the previous section, for a given strain rate (η_1), an increase in vorticity (η_2) results in a decrease in C_μ. This decrease in C_μ is responsible for the additional inhibition of turbulence over that occurring due to reduced production (caused by diminished strain rate due to convex curvature). For concave curvature ($C_f < 0$), the total vorticity is lower resulting in a higher C_μ, and consequently higher turbulence levels. In Figure 2, C_μ is plotted as a function of curvature factor (C_f) for a given value of $S = 6$ which corresponds

to its equilibrium value in rectilinear homogeneous shear flow. In this calculation of C_μ and all the results presented below, the linearized version of the pressure-strain correlation model of Speziale *et al.* [16] is used. It is seen from the figure 2 that the eddy viscosity is a stronger function of convex than concave curvature. This is consistent with the observation of Muck *et al.* [3] who find that turbulence reacts more quickly to convex than concave curvature.

Comparison with other models. Algebraic Reynolds stress models provide an inexpensive alternative to Reynolds stress closure models (RSCM) at the cost of lesser physical accuracy. The closer an algebraic model calculation gets to RSCM calculation, the better the algebraic model. Here, we evaluate the following explicit algebraic models against RSCM calculations: (i) the present curve-sensitive ARSM based on the new weak-equilibrium assumption, CARSM; (ii) the ARSM of Girimaji [9] based on the Rodi-weak equilibrium assumption, ARSM(G); (iii) the ARSM of Gatski and Speziale, ARSM(GS); and (iv) the standard K-ε model.

In Figure 3, we compare the computations from the various models in the stabilizing curvature case ($C_f = 0.15$ and $S(t=0) = 2.0$). The anisotropy components b_{11} and b_{12} are compared in Figure 3a. The RSCM exhibits a gradual growth from zero values of these components to $b_{11} = 0.188$ and $b_{12} = -0.0116$ at the end of the simulation. In rectilinear shear flow, the equilibrium value of b_{12} is approximately -0.157. Therefore, in the present case the turbulent shear stress level is much smaller, indicating a suppression of turbulence production. The algebraic model computations exhibit a sudden jump, on the onset of curved shear, followed by gradual evolution. The CARSM, after a short initial phase ($St \approx 2$), reproduces the behavior of RSCM very accurately. The other models do not reproduce the RSCM results well at all. The performance of ARSM(G) and ARSM(GS) is somewhat better than that of the K-ε model. The K-ε model is, of course, insensitive to curvature and indicates no suppression of turbulence due to stabilizing curvature. The P/ε ratio predicted by the various models is shown in Figure 3b. The RSCM and CARSM are again indistinguishably close after the initial phase. The P/ε at the end of the simulation is about 0.312 (as compared to 1.88 for rectilinear homogeneous shear turbulence), clearly implying a suppression

of turbulence. The other models are not close to RSCM and generally indicate a lesser degree of turbulence suppression.

In Figure 4, the comparison in the destabilizing curvature case ($C_f = -0.15$ and $S(0) = 6.0$) is presented. The RSCM calculations show a clear augmentation of turbulence reflected by higher values of P/ε and $|b_{12}|$. Again, the present CARSM captures RSCM behavior extremely well. The other models do not duplicate the RSCM behavior as accurately.

From the above figures it is quite clear that the present CARSM is an excellent alternative to RSCM for curved homogeneous shear flows. The other algebraic models while not too bad for destabilizing curvature perform poorly for stabilizing curvature.

Validation against experimental data. The CARSM is now validated against the curved homogeneous shear flow data of Holloway and Tavoularis [17]. The experimental equilibrium values of b_{12} and P/ε ratio are compared against CARSM calculations for various curvature factors. In order to isolate the present model comparison from the well-known shortcomings of the dissipation equation (Speziale *et al.* [16]), the experimental value of the ϵ-dependent normalized shear rate is used. The normalized shear rate values taken from the experiment for various curvature factors are given in Table 1.

Comparison is performed only for those cases which attain structural equilibrium in the experiment. Calculations from the standard K-ε model are also presented. Figure 5 shows the comparison of shear stress anisotropy, b_{12}. As is to be expected, the experimental data shows increased shear stress magnitudes for negative curvature factors (destabilizing curvature) and diminished values for positive curvature factors (stabilizing curvature). The curved algebraic Reynolds stress model captures this variation as a function of curvature reasonably well. On the whole, the CARSM appears to slightly overpredict the shear stress levels for destabilizing curvatures and suppress the shear stress a little more than indicated by data for stabilizing curvatures. The standard K-ε model, on the other hand, predicts much higher levels of shear stress for all curvatures.

One of the key issues that needs to be predicted with accuracy in curved turbulent flows is the re-

laminarization effect induced by stabilizing curvature. In a plane homogeneous shear flow, the turbulence production is greater than dissipation, $P \approx 1.8\varepsilon$, resulting in an exponential growth of turbulent kinetic energy. When the flow encounters convex curvature, the production decreases due to reduced levels of turbulent viscosity and effective strain rate, resulting in slower growth of the turbulent kinetic energy. When the convex curvature is strong enough, the turbulence production becomes smaller than dissipation resulting in the decay of kinetic energy. The value of the curvature factor at which this kinetic energy decay (interpreted as onset of relaminarization) begins is of great interest. The equilibrium values of P/ε are compared in Figure 6. Whereas both of the models capture the correct trend of decreasing production with increasing curvature factor, the CARSM values are much closer to the experimental data.

For a fully developed homogeneous curved shear flow with circular streamlines, the weak-equilibrium assumption invoked in this paper is an exact statement. Since the flow is homogeneous, the neglect of the turbulent transport term in the ARSM methodology is also completely valid. This begs the question, why is there still a distinct discrepancy between the model and experimental data? If the experimental results are reliable, the lack of complete agreement between the experiment and CARSM must be due to the pressure-strain correlation model. The pressure-strain correlation models have generally been optimized for non-curved homogeneous flows. If one were to use a nonlinear pressure-strain model, a fully explicit, self-consistent ARSM may not be possible. This calls for the development of quasilinear pressure-strain correlation models (of the form given in equation 24) that are optimized for curved homogeneous flows. (A fully nonlinear model derived specifically for rotating and curved flows is presented in Ristorcelli *et al.* [18]).

5 Conclusion

A new weak-equilibrium hypothesis for flows with streamline curvature has been proposed and developed. This hypothesis ensures Galilean invariance and is also consistent with known physics of circular flows. In the absence of streamline curvature, the hypothesis reduces to the Rodi weak-equilibrium assumption. Employing the new assumption, an explicit and self-consistent algebraic Reynolds stress model is derived

from the Reynolds stress transport equation. This model expression is the analytical fixed point solution of the anisotropy evolution equation in two-dimensional flows for a variety of quasilinear pressure-strain correlation models. The algebraic model computations are validated against Reynolds stress closure model (RSCM) computations and experimental data (of Holloway and Tavoularis [17]) in curved homogeneous shear flows. The agreement is excellent with RSCM and adequate with experimental data.

References

[1] P. Bradshaw, *The analogy between streamline curvature and buoyancy in turbulent flow*, J. Fluid Mech. **36**, 177–191, (1969).

[2] P. Bradshaw, *The effects of streamline curvature on turbulent flow*, AGARDograph no. 169 (1973).

[3] K. C. Muck, P. H. Hoffman, and P. Bradshaw, *The effect of convex surface curvature on turbulent boundary layers*, J. Fluid Mech. **161**, 347–369, (1985).

[4] P. H. Hoffman, K. C. Muck, and P. Bradshaw, *The effect of concave surface curvature on turbulent boundary layers*, J. Fluid Mech. **161**, 371–403, (1985).

[5] W. Rodi, *A New Algebraic Relation for Calculating Reynolds Stress*, (ZAMM) **56**, T219–T221, (1976).

[6] S. B. Pope, *A More General Effective-Viscosity Hypothesis*, J. Fluid Mech. **72**, 331–340, (1975).

[7] D. B. Taulbee, *An improved algebraic stress model and corresponding nonlinear stress model*, Phys. Fluids A **4**, 2555–2561, (1992).

[8] T. B. Gatski and C. G. Speziale, *On explicit algebraic stress models for complex turbulent flows*, J. Fluid Mech. **254**, 59–78, (1993).

[9] S. S. Girimaji, *Fully Explicit and Self-Consistent Algebraic Reynolds Stress Model*, ICASE Report No. 95-82. Also submitted to the J. Fluid Mech. for publication.

[10] S. Eskinazi and H. Yeh, *An Investigation of Fully Developed Turbulent Flows in a Curved Channel*, J. of the Aeronautical Sciences **13**, 23–34, (1956).

[11] R. D. Moser and P. Moin, *The effect of curvature on wall-bounded turbulent flows*, J. Fluid Mech. **175**, 479–510, (1987).

[12] W. Rodi and G. Scheurer, *Calculations of Curved Shear Layers with Two Equation Turbulence Models*, Phys. Fluids **26**(6), 1422–1436, (1983).

[13] B. A. Younis, Ph.D. Thesis, University of London, (1984).

[14] S. S. Girimaji, *An Algebraic Stress Model For Curved Flows.* Master's Thesis, Cornell University (1986).

[15] S. Fu, P. G. Huang, B. E. Launder, and M. A. Leschziner, *A Comparison of Algebraic and Differential Second-Moment Closure for Axisymmetric Turbulent Shear Flows With and Without Swirls*, J. Fluids Engng. **110**, 216, (1988).

[16] C. G. Speziale, S. Sarkar, and T. B. Gatski, *Modeling the pressure-strain correlation of turbulence: An invariant dynamical system approach*, J. Fluid Mech. **227**, 245–272, (1991).

[17] A. G. L. Holloway and S. Tavoularis, *The effects of turbulence on sheared turbulence*, J. Fluid Mech. **237**, 569–603, (1992).

[18] J. R. Ristorcelli, J. L. Lumley, and R. Abid, *A rapid pressure covariance representation consistent with the Taylor-Proudman theorem materially indifferent in the two-dimensional limit* J. Fluid Mech. **292**, 111–152, (1995).

Table 1: Table of Parameters

	Cases											
	1	2	3	4	5	6	7	8	9	10	11	12
S	4.7	4.6	4.26	5.85	6.54	5.66	4.58	3.89	3.14	4.17	3.63	3.10
C_f	-0.033	-0.039	-0.066	-0.079	-0.093	-0.150	0.032	0.040	0.076	0.078	0.10	0.18

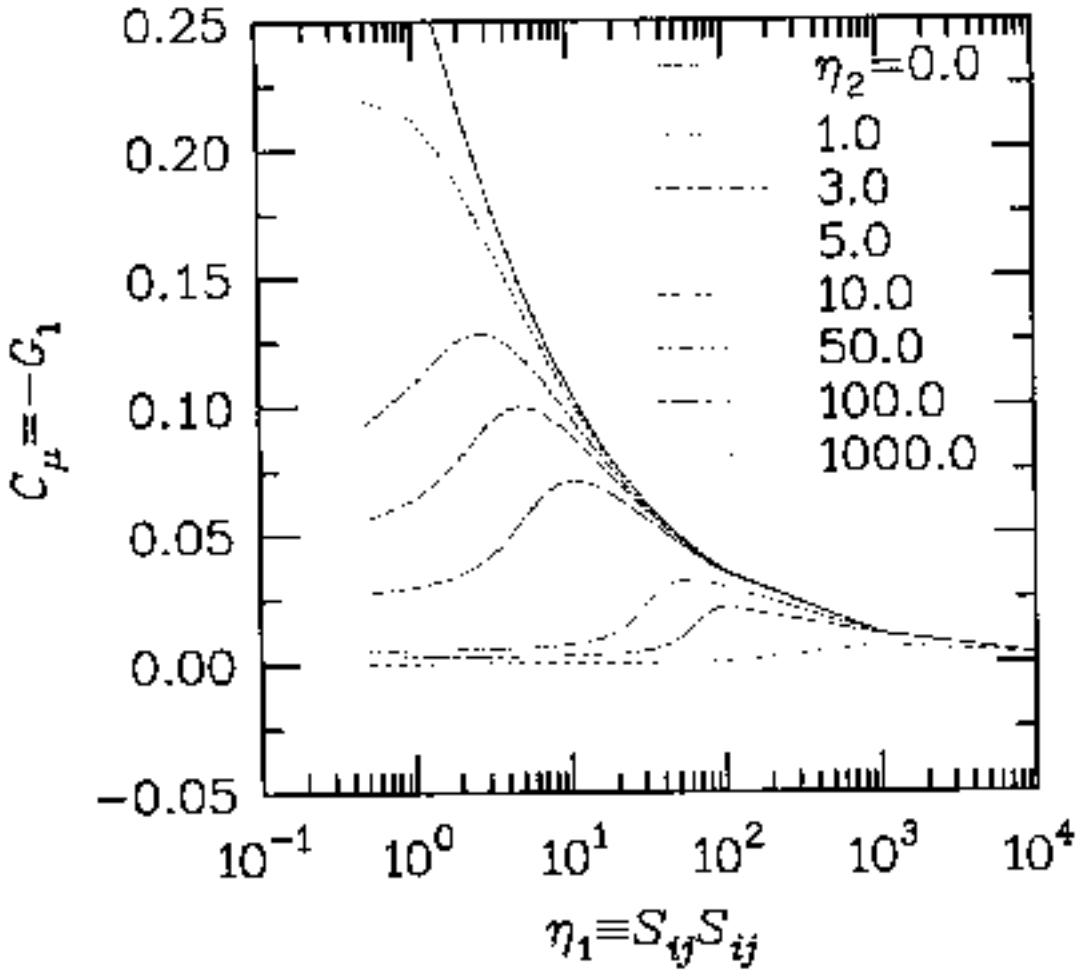

Figure 1: C_μ as a function of η_1 and η_2.

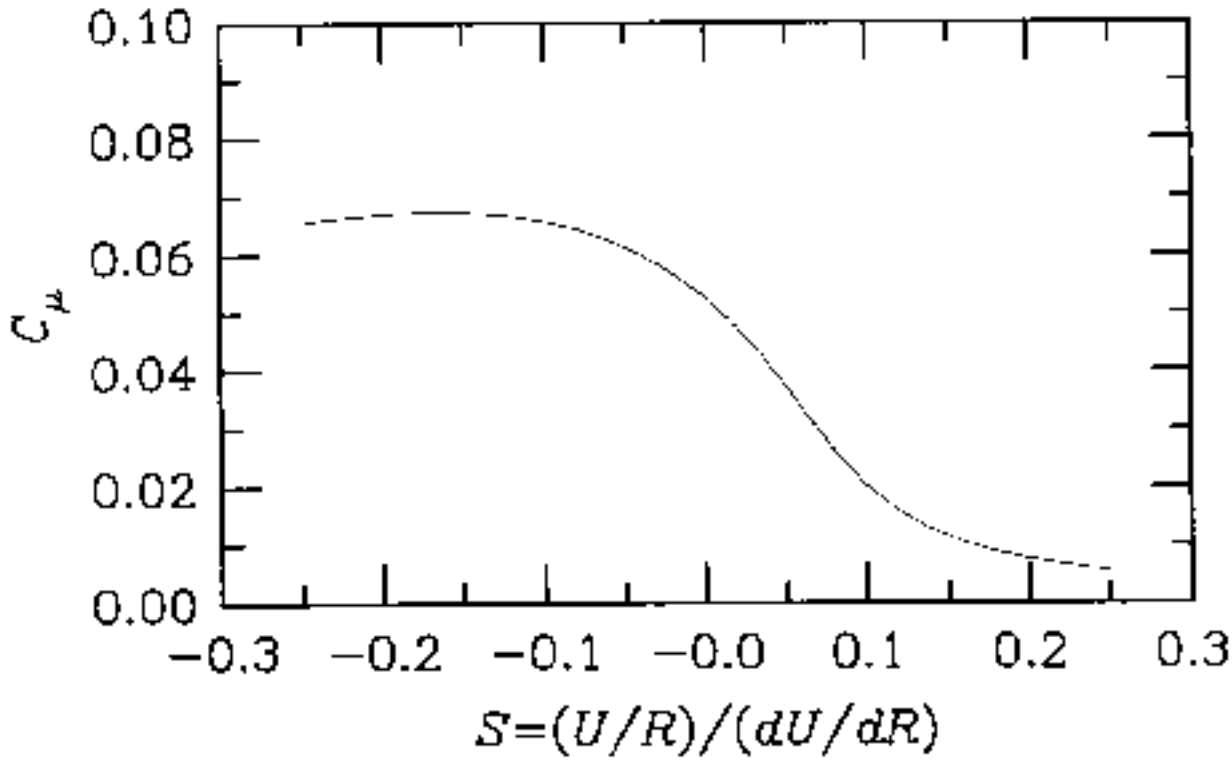

Figure 2: C_μ as a function of C_f in curved homogeneous shear flow. $S = (\partial U/\partial r)(K/\varepsilon) = 6.0$

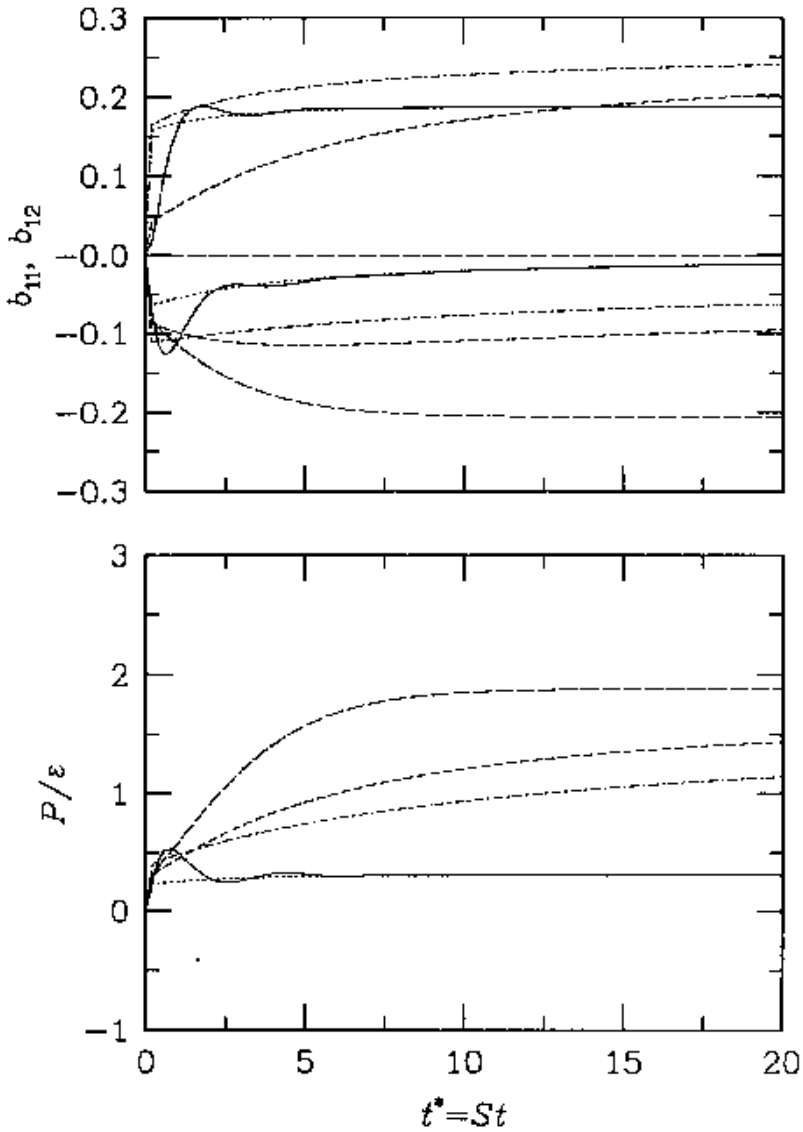

Figure 3: Comparison between Reynolds Stress Closure Model and other models in the curved homogeneous shear flow case $C_f = 0.15$: — RSCM; - - Curved ARSM; – - – ARSM(G); – – ARSM(GS); and — — K-ε model.

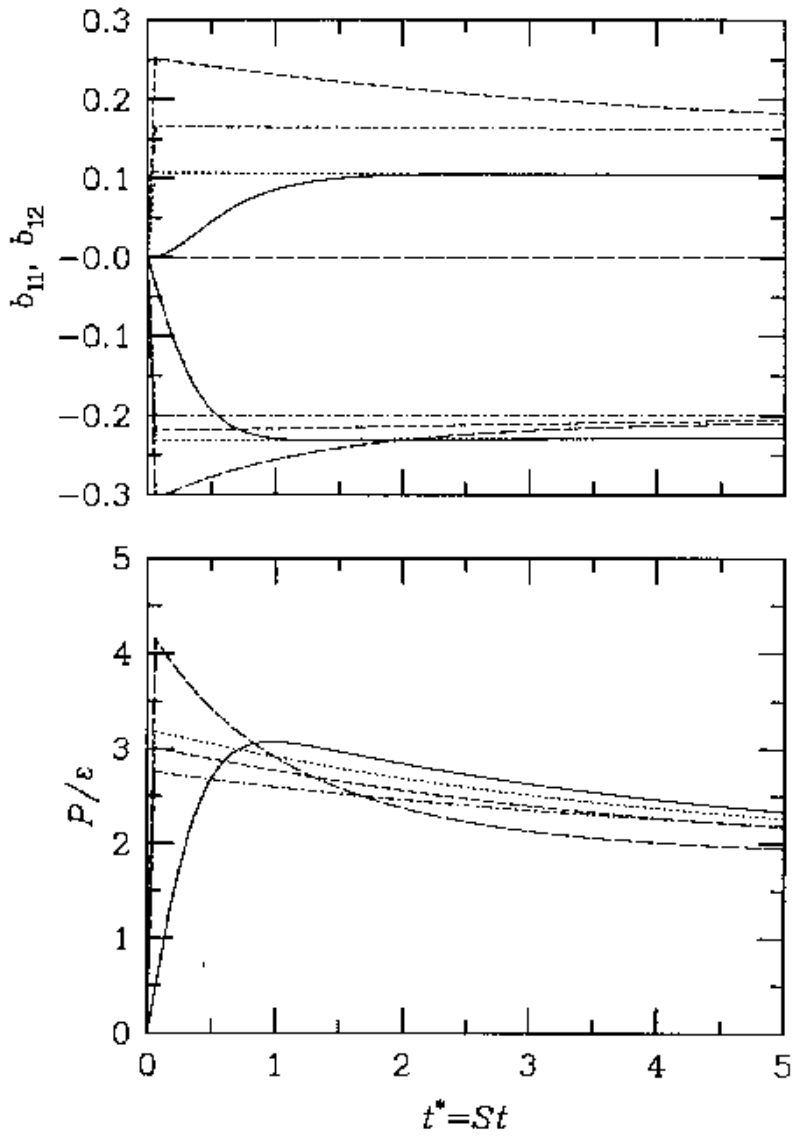

Figure 4: Comparison between Reynolds Stress Closure Model and other models in the curved homogeneous shear flow case $C_f = -0.15$. (Legend same as Figure 3.)

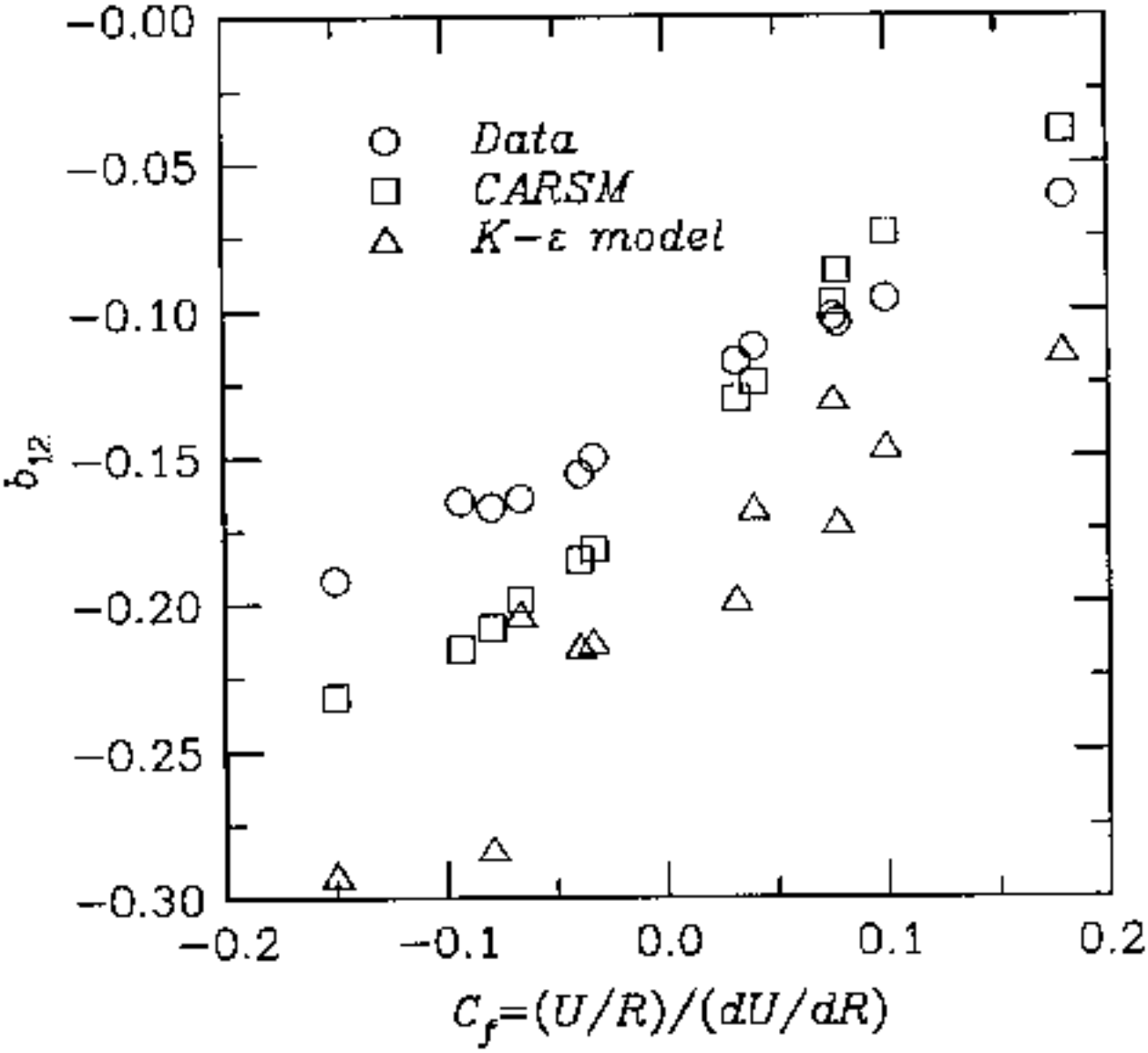

Figure 5: Comparison between experimental data, ARSM, and standard K-ε model: anisotropy of shear stress, b_{12}.

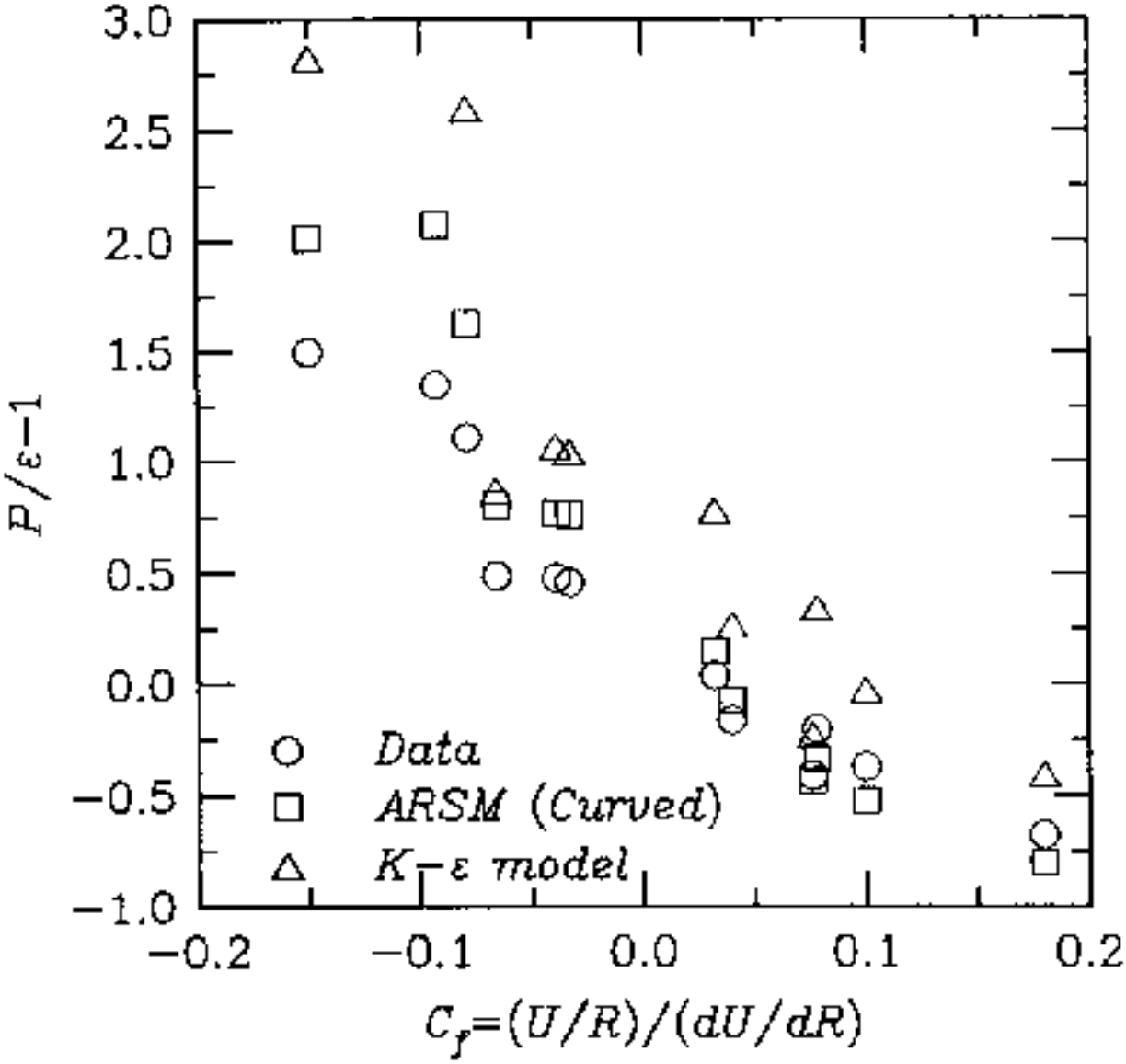

Figure 6: Comparison between experimental data, ARSM, and standard K-ε model: production to dissipation ratio.